Eur. Phys. J. C (2022) 82:755
https://doi.org/10.1140/epjc/s10052-022-10715-0

THE EUROPEAN PHYSICAL JOURNAL C

Letter

Back-to-back azimuthal correlations in Z+jet events at high transverse momentum in the TMD parton branching method at next-to-leading order

H. Yang[1,2], A. Bermudez Martinez[2], L. I. Estevez Banos[2], F. Hautmann[3,4,5], H. Jung[2,a], M. Mendizabal[2], K. Moral Figueroa[6], S. Prestel[7], S. Taheri Monfared[2], A. M. van Kampen[4], Q. Wang[1,2], K. Wichmann[2]

[1] School of Physics, Peking University, Beijing, China
[2] Deutsches Elektronen-Synchrotron DESY, Hamburg, Germany
[3] Theoretical Physics Department, CERN, Geneva, Switzerland
[4] Elementary Particle Physics, University of Antwerp, Antwerp, Belgium
[5] University of Oxford, Oxford, UK
[6] University of Edinburgh, Edinburgh, UK
[7] Department of Astronomy and Theoretical Physics, Lund University, Lund, Sweden

Received: 7 April 2022 / Accepted: 16 August 2022

Abstract Azimuthal correlations in Z+jet production at large transverse momenta are computed by matching Parton-Branching (PB) TMD parton distributions and showers with NLO calculations via MCatNLO. The predictions are compared with those for dijet production in the same kinematic range. The azimuthal correlations $\Delta\phi$ between the Z boson and the leading jet are steeper compared to those in dijet production at transverse momenta $\mathcal{O}(100)$ GeV, while they become similar for very high transverse momenta $\mathcal{O}(1000)$ GeV. The different patterns of Z+jet and dijet azimuthal correlations can be used to search for potential *factorization-breaking* effects in the back-to-back region, which depend on the different color and spin structure of the final states and their interferences with the initial states. In order to investigate these effects experimentally, we propose to measure the ratio of the distributions in $\Delta\phi$ for Z+jet- and multijet production at low and at high transverse momenta, and compare the results to predictions obtained assuming factorization. We examine the role of theoretical uncertainties by performing variations of the factorization scale, renormalization scale and matching scale. In particular, we present a comparative study of matching scale uncertainties in the cases of PB-TMD and collinear parton showers.

1 Introduction

The description of jet production in association with a Z boson in hadron–hadron collisions is an important test of predictions obtained in Quantum Chromodynamics (QCD), and provides a relevant background to Higgs boson studies and to new physics searches. The associated Z boson plus jet production has been measured by CDF and D0 in proton-antiproton collisions at a center-of-mass energy $\sqrt{s} = 1.96$ TeV [1,2]. At the LHC, the ATLAS and CMS collaborations have published measurements in proton-proton (pp) collisions at a center-of-mass energy $\sqrt{s} = 7$ TeV [3–5], 8 TeV [6] and 13 TeV [7,8]. Azimuthal correlations between Z bosons and jets have been measured at 8 TeV [6] and 13 TeV [8].

The distribution in the azimuthal angle $\Delta\phi$ between the Z boson and the jet is an especially sensitive observable, probing several aspects of QCD physics. At leading order in the strong coupling α_s, one has $\Delta\phi = \pi$. The smearing of this delta-like distribution is a measure of higher order QCD radiation. In the region near $\Delta\phi = \pi$, this is primarily soft gluon radiation, while in the region of small $\Delta\phi$ it is primarily hard QCD radiation. The large-$\Delta\phi$ region of nearly back-to-back Z boson and jet is influenced by both perturbative and non-perturbative QCD contributions. The relative significance of these contributions depends on the scale of the transverse momentum imbalance between the boson and the jet. Importantly, the resummation of soft multi-gluon emissions in the nearly back-to-back region probes the transverse momenta

[a] e-mail: hannes.jung@desy.de (corresponding author)

Published online: 29 August 2022

of the initial state partons, which can be described by transverse momentum dependent (TMD) [9] parton distribution functions (PDFs). Theoretical predictions for Z boson + jet production including soft gluon resummation have recently been given in Refs. [10–16].

All the experimental measurements of boson–jet azimuthal correlations that have been performed so far are in the kinematical range of transverse momenta of the Z boson and the jets of the order $p_{\mathrm{T}} \approx \mathcal{O}(100)$ GeV. In this kinematical range, fixed-order perturbative corrections beyond next-to-leading order (NLO) are sizeable, and at small $\Delta\phi$ NLO calculations are usually not sufficient for reliable predictions. For the large-$\Delta\phi$ region of nearly back-to-back Z boson and jet, the boson–jet p_{T} imbalance scale is of order a few GeV, which is significantly influenced by both perturbative resummation and non-perturbative effects. It is worth noting that all the experimental measurements performed up to now do not cover the large $\Delta\phi$, nearly back-to-back, region with sufficiently fine binning to investigate detailed features of QCD.

With the increase in luminosity at the LHC, it becomes possible to measure Z+jet production in the high p_{T} range, with $p_{\mathrm{T}} \approx \mathcal{O}(1000)$ GeV. In this work, we observe that in this kinematical range the resummation of soft gluons and TMD dynamics in the nearly back-to-back region can be explored in a new regime, characterized by boson–jet p_{T} imbalance scales on the order of a few ten GeV. The large-$\Delta\phi$ region, involving deviations of the order of the experimental angular resolution of about 1 degree from $\Delta\phi = \pi$, can be investigated by analyzing jets with measurable transverse momenta.

Based on the above observation, in this paper we propose experimental investigations of back-to-back azimuthal correlations in the $p_{\mathrm{T}} \approx \mathcal{O}(1000)$ GeV region, with a systematic scan of the large-$\Delta\phi$ regime from this high p_{T} region down to $p_{\mathrm{T}} \approx \mathcal{O}(100)$ GeV – a regime which is completely unexplored experimentally up to now. We present dedicated phenomenological studies of this $\Delta\phi$ region as a function of p_{T}, enabling one to explore boson–jet transverse momentum imbalances from a jet scale of several ten GeV down to the few GeV scale. To perform these studies, we use the Parton Branching (PB) approach [17,18] to TMD evolution, matched to NLO calculations of Z+jet production with MadGraph5_aMC@NLO [19]. This approach has already been successfully applied, across a wide energy and mass range, to the Z boson p_{T} spectrum at the LHC [20] and the Drell–Yan (DY) p_{T} spectrum at lower fixed-target energies [21], so that the investigation of the same method in the Z+jet case is compelling. The $\Delta\phi$ correlation in the kinematical range proposed in this paper allows one to study the interplay of perturbative and non-perturbative contributions to TMD dynamics (see e.g. [22] for the DY case) as a function of both the boson–jet p_{T} imbalance and the evolution scale of the TMD distribution itself, of the order of the hard scale of the process, given by the transverse momenta of the Z boson or the jet.

In a previous publication [23] we have investigated the $\Delta\phi_{12}$ correlation in high-p_{T} dijet events by applying TMD PDFs and parton shower together with NLO calculations of the hard scattering process. In multijet events the azimuthal correlation between two jets has been measured at the LHC by ATLAS and CMS [24–28]. The region of $\Delta\phi_{12} \to \pi$ is of special interest, since so-called *factorization-breaking* [29–31] effects could become important in the case of colored final states. Multijet production is believed to be sensitive to such effects, as well as vector boson + jet production [32]. In order to investigate factorization-breaking effects, we propose to compare the theoretical description of the azimuthal correlation $\Delta\phi_{12}$ in multijet production with the one in Z+jet production. A thorough investigation of azimuthal correlations in the back-to-back region in Z+jet events has been also performed in Ref. [11], addressing the issue of factorization-breaking.

In this report we compare in detail high-p_{T} dijet and Z+jet production by applying the PB TMD method [17,18] matched with NLO. In Ref. [23] the NLO PB TMD predictions have been found to describe well the measurements of dijet azimuthal correlations [27,28]. In the present paper we apply the same method to the calculation of Z+jet production, and present the corresponding predictions. We propose to use the same kinematic region for the high-p_{T} dijet and Z+jet production to allow a direct comparison of the angular observables in the two cases.

We will see that, in the region of leading transverse momenta of the order $p_{\mathrm{T}} \approx \mathcal{O}(100\ \mathrm{GeV})$, the boson–jet final state is more strongly correlated azimuthally than the jet–jet final state. As the transverse momenta increase above the electroweak symmetry breaking scale, $p_{\mathrm{T}} \approx \mathcal{O}(1000\ \mathrm{GeV})$, this difference is reduced, and the boson–jet and jet–jet become more similarly correlated. We connect this behavior to features of the partonic initial state and final state radiation in the boson–jet and jet–jet cases. Since potential factorization-breaking effects arise from color interferences of initial-state and final-state radiation, different breaking patterns can be expected for strong and weak azimuthal correlations, influencing differently the boson–jet and jet–jet cases. We therefore propose to systematically compare measurements of dijet and Z+jet distributions, scanning the phase space from low transverse momenta $p_{\mathrm{T}} \approx \mathcal{O}(100\ \mathrm{GeV})$ to high transverse momenta $p_{\mathrm{T}} \approx \mathcal{O}(1000\ \mathrm{GeV})$.

In the following, we start by describing the basic elements of the PB TMD method and the Z+jet calculation in Sect. 2. In Sect. 3 we present results for the Z+jet azimuthal correla-

tions and compare them with the multijet case. We summarize in Sect. 4. In an Appendix we discuss technical details on the use of MCatNLO+CASCADE3.

2 Basic elements of the calculation

In this section we first recall the salient features of the PB TMD approach, summarizing the main concepts of the approach and its applications; then we describe the calculation of Z+jet production by the PB TMD method matched with NLO matrix elements in MADGRAPH5_AMC@NLO.

2.1 PB-TMD method

The PB approach [18] provides a formulation for the evolution of TMD parton distributions in terms of perturbatively calculable Sudakov form factors and real-emission splitting kernels, with angular ordering phase space constraints and with non-perturbative distributions at the initial scale of the evolution to be determined from fits to experiment. This formulation uses a soft-gluon resolution scale z_M [17] to separate resolvable and non-resolvable branchings. An important feature of the PB TMD evolution equation [18] concerns its collinear limits: upon integration over all transverse momenta, the PB TMD evolution equation returns the DGLAP [33–36] equation for resolution scale $z_M \to 1$, while it coincides with the CMW [37,38] coherent branching equation for angular-ordered z_M [39]. The PB TMD method is based on the "unitarity" picture [40] of parton evolution usually employed in parton showering Monte Carlo (MC) algorithms [41,42]. The PB evolution equation for the TMD distributions is matched by a corresponding TMD parton shower for the spacelike parton cascade, generated by "backward evolution" [43]. A significant difference with respect to ordinary parton showers is that in the PB TMD method TMD distributions are defined and determined from fits to experimental data, which places constraints on fixed-scale inputs to evolution, while in ordinary parton showers instead non-perturbative physics parameters and showering parameters are tuned. No MC tuning is performed in the PB TMD case.

The NLO PB collinear and TMD parton distributions were obtained in Ref. [44] from QCD fits to precision DIS data from HERA [45] using the xFitter analysis framework [46,47]. Two different sets, PB-NLO-2018-Set 1 and PB-NLO-2018-Set 2, were obtained, with PB-NLO-2018-Set 1 corresponding at collinear level to HERAPDF 2.0 NLO [45]. In PB-NLO-2018-Set 2 the transverse momentum (instead of the evolution scale in Set 1) is used as the scale in the running coupling α_s which corresponds to the angular ordering of soft gluon emissions in the initial-state parton evolution [38,39,48,49]. It has been shown in [20,21] that Set 2 provides a better description of experimental measurements for the Z-boson spectrum at low-p_T. Also, it has been shown in [23] that the transverse momentum scale in the running coupling α_s is important for a good description of data on di-jet angular correlations. In this paper we will concentrate on Set 2 only.

In Fig. 1 we show the TMD PDF distributions for up quarks and gluons at $x = 0.01$ and $\mu = 100$ and 1000 GeV for PB-NLO-2018-Set 2. The transverse momentum distribution of gluons is broader than that of quarks, due to gluon self-coupling and the different color factors. In Fig. 1 also the uncertainties of the distributions, as obtained from the fit [44], are shown. The differences in the transverse momentum spectra of quarks and gluons will show up in differences in azimuthal correlation distributions.

The PB TMD evolution equation resums Sudakov logarithms. Current calculations in the PB TMD approach are performed with leading-logarithm (LL) and next-to-leading-logarithm (NLL) accuracy. The accuracy can be systematically improved, and the extension to next-to-next-to-leading logarithmic (NNLL) accuracy is being studied. In this respect, the approach can be compared [50] with analytic resummation methods [51,52]. The extraction of TMD distributions from the PB TMD fits described above could be compared with extractions, such as [53,54], based on [51,52]. The TMDlib tool [55,56] is designed as an aid for such studies. On the other hand, while analytic resummation approaches apply to the inclusive transverse momentum spectrum, the PB TMD approach works at exclusive level and can be applied to make predictions not only for the inclusive spectrum but also for the structure of the final states.

A framework to compute theoretical predictions combining the PB TMD resummation with fixed-order NLO matrix elements in MADGRAPH5_AMC@NLO has been developed in [20,21]. The predictions [20] have been successfully compared with LHC measurements of Z boson p_T and ϕ^* distributions [57–59]. Predictions by this method have also been successful in describing [21] DY p_T spectra at lower masses and energies [60–63]. The significance of this result is enhanced by the recent observation [64] that fixed-order NNLO corrections are not extremely large in the kinematic region of the data. This framework has also been applied to di-jet production [23], and predictions for di-jet correlations have been found in good agreement with LHC measurements [27,28]. We will employ this framework for Z+jet production in the next subsection.

As a method which is applicable at the level of exclusive final states, the PB TMD approach can be used in the context of multi-jet merging algorithms. A TMD multi-jet merging method has been developed in [65]. Its application to Z boson + multi-jets production [65–67] illustrates that trans-

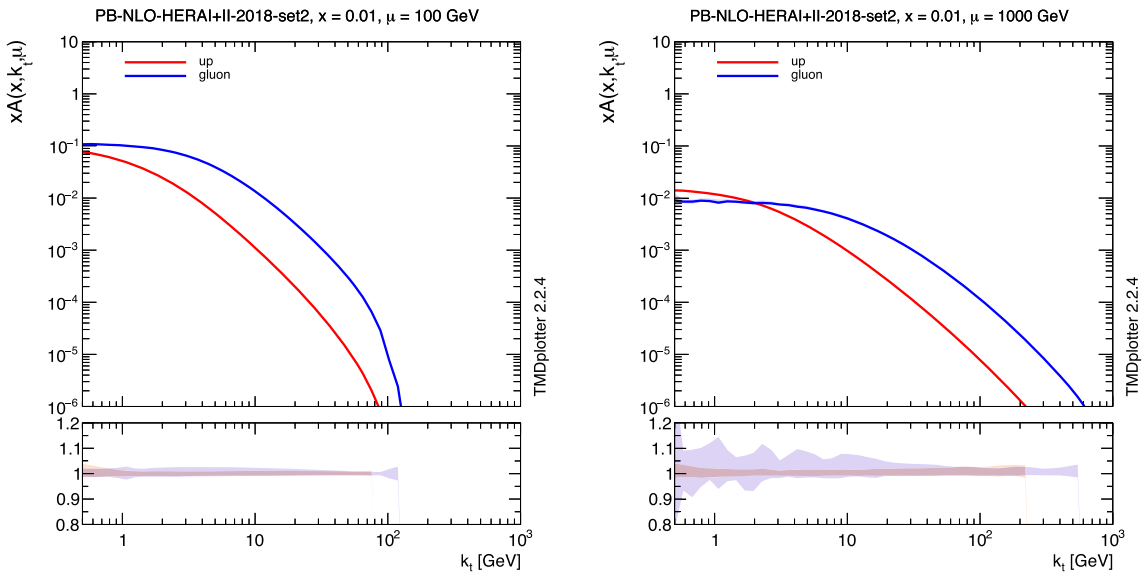

Fig. 1 TMD parton density distributions for up quarks and gluons of PB-NLO-2018-Set 2 as a function of k_T at $\mu = 100$ and 1000 GeV and $x = 0.01$. In the lower panels show the full uncertainty of the TMD PDFs, as obtained from the fits [44]

verse momentum recoils in the initial-state showers [68–70] influence significantly the theoretical systematics associated with the merging parameters. In the present paper, we will concentrate on the Z+jet back-to-back region, rather than the multi-jet production region, and we will therefore not use the TMD merging procedure.

Recently, the PB TMD evolution equation has been generalized to include TMD splitting functions [71,72], defined through high-energy factorization [73]. This generalization is important particularly for processes sensitive to TMD distributions at small values of longitudinal momentum fractions x. In this paper we focus on processes at mid to large x, and thus we do not consider this in the following.

2.2 Calculation of Z+jet distributions

The process Z+jet at NLO is calculated with MADGRAPH5_AMC@NLO using the collinear PB-NLO-2018-Set 2, as obtained in Ref. [44] applying $\alpha_s(M_Z) = 0.118$. The matching of NLO matrix elements with PB TMD parton distributions is described in Refs. [20,21,43]. The extension to multijet production is illustrated in Ref. [23]. Predictions are obtained by processing the MADGRAPH5_AMC@NLO event files in LHE format [74] through CASCADE3 [43] for an inclusion of TMD effects in the initial state and for simulation of the corresponding parton shower (labeled MCatNLO+CAS3 in the following).

Fixed order NLO Z+jet production is calculated with MADGRAPH5_AMC@NLO in a procedure similar to the one applied for dijet production described in [23] (labeled MCatNLO(fNLO)). For the MCatNLO mode, the HERWIG6 [75,76] subtraction terms are calculated, as they are best suited for the use with PB-parton densities, because both apply the same angular ordering condition. The use of HERWIG6 subtraction terms together with CASCADE3 is justified in the Appendix for final state parton shower as well as initial and final state showers by a comparison of the predictions obtained with CASCADE3 and with HERWIG6. The matching scale $\mu_m =$ SCALUP limits the contribution from PB-TMDs and TMD showers.

In the calculations, the factorization and renormalization scales are set to $\mu = \frac{1}{2}\sum_i p_{T,i}$, where the index i runs over all particles in the matrix element final state. This scale is also used in the PB-TMD parton distribution $\mathcal{A}(x, k_T, \mu)$. The scale uncertainties of the predictions are obtained from variations of the scales around the central value in the 7-point scheme avoiding extreme cases of variation.

In Fig. 2 we show the distributions of the transverse momentum of the Z+jet system, $p_{T,Zj}$, and the azimuthal correlation in the Z+jet system, $\Delta\phi_{Zj}$, for a fixed NLO calculation, for the full simulation including PB-TMD PDFs and parton showers as well as for the MCatNLO calculation at the level where subtraction terms are included without addition from parton shower (LHE-level). We require a transverse momentum $p_T > 200$ GeV for the Z boson and define jets with the anti-k_T jet-algorithm [77], as implemented in the FASTJET package [78], with a distance parameter of R = 0.4. The effect of including PB-TMD PDFs and parton showers can be clearly seen from the difference to the fixed NLO and LHE-level calculations.

In the low $p_{T,Zj}$ region one can clearly see the expected steeply rising behavior of the fixed NLO prediction. In the $\Delta\phi_{Zj}$ distribution one can observe the limited region for fixed NLO at $\Delta\phi_{Zj} < 2/3\pi$, since at most two jets in

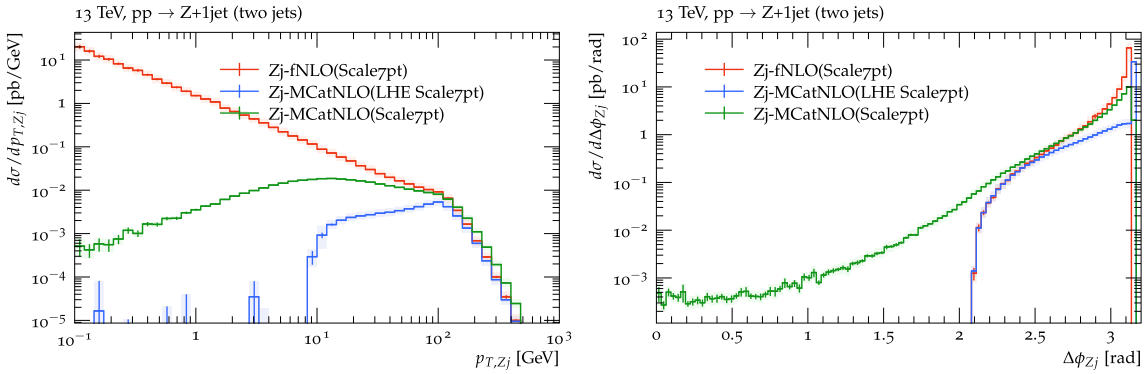

Fig. 2 Transverse momentum spectrum of the Z+jet-system $p_{\mathrm{T},Zj}$ (left) and $\Delta\phi_{\mathrm{Zj}}$ distribution (right). Shown are predictions from fixed NLO (fNLO), the (unphysical) distribution at LHE-level and the full simulation (after inclusion of PB-TMDs and TMD showers, MCatNLO+CAS3)

addition to the Z boson appear in the calculation. At large $\Delta\phi_{\mathrm{Zj}}$, the fixed NLO prediction rises faster than the full calculation including resummation via PB-TMDs and parton showers. In the following we concentrate on the large $\Delta\phi_{\mathrm{Zj}}$ region.

3 Back-to-back azimuthal correlations in Z+jet and multijet production

We now present predictions, obtained in the framework described above, for Z+jet and multijet production.[1] The selection of events follows the one of azimuthal correlations $\Delta\phi_{12}$ in the back-to-back region ($\Delta\phi_{12} \to \pi$) in multijet production at $\sqrt{s} = 13$ TeV as obtained by CMS [28]: jets are reconstructed with the anti-k_{T} algorithm [77] with a distance parameter of 0.4 in the rapidity range of $|y| < 2.4$. We require either two jets with $p_{\mathrm{T}}^{\mathrm{leading}} > 200$ GeV or a Z boson and a jet as leading or subleading objects with a transverse momentum $p_{\mathrm{T}}^{\mathrm{leading}} > 200$ GeV.

We consider distributions of the azimuthal correlation between the Z boson and the leading jet, $\Delta\phi_{\mathrm{Zj}}$, for $p_{\mathrm{T}}^{\mathrm{leading}} > 200$ GeV as well as for the very high p_{T} region of $p_{\mathrm{T}}^{\mathrm{leading}} > 1000$ GeV.

The calculations are performed with MCatNLO+CAS3 using PB-NLO-2018-Set 2 as the collinear and TMD parton densities with running coupling satisfying $\alpha_{\mathrm{s}}(m_{\mathrm{Z}}) = 0.118$ and PB-TMD parton shower.

In Fig. 3, the prediction for the azimuthal correlations $\Delta\phi_{\mathrm{Zj}}$ for Z+jet production in the back-to-back region is shown.[2] We also show, for comparison, the prediction of azimuthal correlations $\Delta\phi_{12}$ for multijet production in the same kinematic region, compared to the measurement of dijet production obtained by CMS [28]. We observe that the distribution of azimuthal angle $\Delta\phi_{\mathrm{Zj}}$ in Z+jet-production for $p_{\mathrm{T}}^{\mathrm{leading}} > 200$ GeV is more strongly correlated towards π than the distribution of angle $\Delta\phi_{12}$ in multijet production. This difference is reduced for $p_{\mathrm{T}}^{\mathrm{leading}} > 1000$ GeV.

Differences in $\Delta\phi$ between Z+jet and multijet production can result from the different flavor composition of the initial state and therefore different initial state transverse momenta and initial state parton shower, as well as from differences in final state showering since both processes have a different number of colored final state partons. Effects coming from factorization-breaking, interference between initial and final state partons, will depend on the final state structure and the number of colored final state partons.

We first investigate the role of initial state radiation and the dependence on the transverse momentum distributions coming from the TMD PDFs, which gives a large contribution to the decorrelation in $\Delta\phi$. The k_{T}-distribution obtained from a gluon TMD PDF is different from the one of a quark TMD PDF as shown in Fig. 1 for $x = 0.01$ and scales of $\mu = 200(1000)$ GeV. In Fig. 4 we show the probability of gg, qg and qq initial states (q stands for quark and antiquark) as a function of $p_{\mathrm{T}}^{\mathrm{leading}}$ for Z+jet and multijet production obtained with MCatNLO+CAS3. At high $p_{\mathrm{T}}^{\mathrm{leading}} > 1000$ GeV the qq channel becomes important for both Z+jet and multijet final states, while at lower $p_{\mathrm{T}}^{\mathrm{leading}} > 200$ GeV the gg channel is dominant in multijet production, leading to larger decorrelation effects, since gluons radiate more compared to quarks.

The role of final state radiation in the correlation in $\Delta\phi_{12}$ distributions is more difficult to estimate, since the subtraction terms for the NLO matrix element calculation also depend on the structure of the final state parton shower. In order to estimate the effect of final state shower we compare a calculation of the azimuthal correlations in the back-to-back region obtained with MCatNLO+CAS3 with the one obtained with MCatNLO+PYTHIA8 (Fig. 5). For the calcula-

[1] A framework based on CCFM evolution [79] was described in [80,81] for multi-jet and vector boson + jet correlations.

[2] Predictions for the region of small $\Delta\phi$ require including the contribution of higher parton multiplicities, e.g. via multi-jet merging [65].

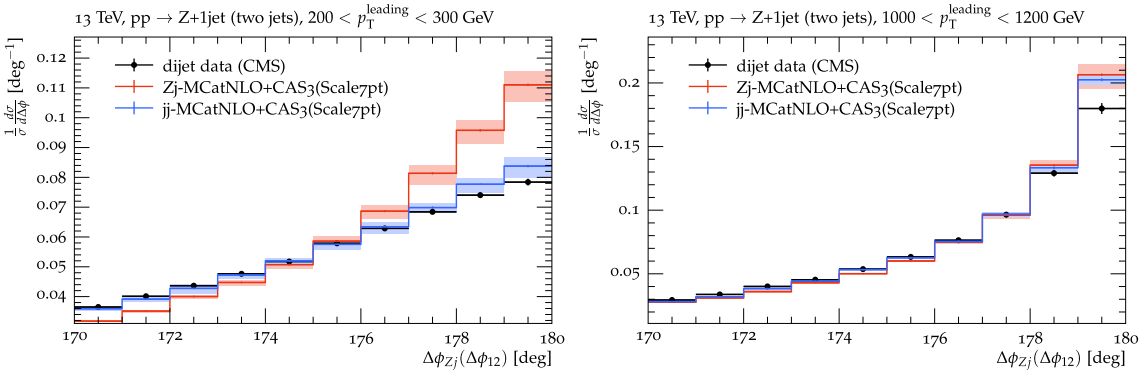

Fig. 3 Predictions of the azimuthal correlation $\Delta\phi_{\mathrm{Zj}}(\Delta\phi_{12})$ for Z+jet and multijet processes in the back-to-back region for $p_{\mathrm{T}}^{\mathrm{leading}} > 200$ GeV (left) and $p_{\mathrm{T}}^{\mathrm{leading}} > 1000$ GeV (right) obtained from MCatNLO+CAS3. Shown are the uncertainties obtained from scale variation (as described in the text). The measurements of dijet correlations as obtained by CMS [28] are shown as data points, for comparison

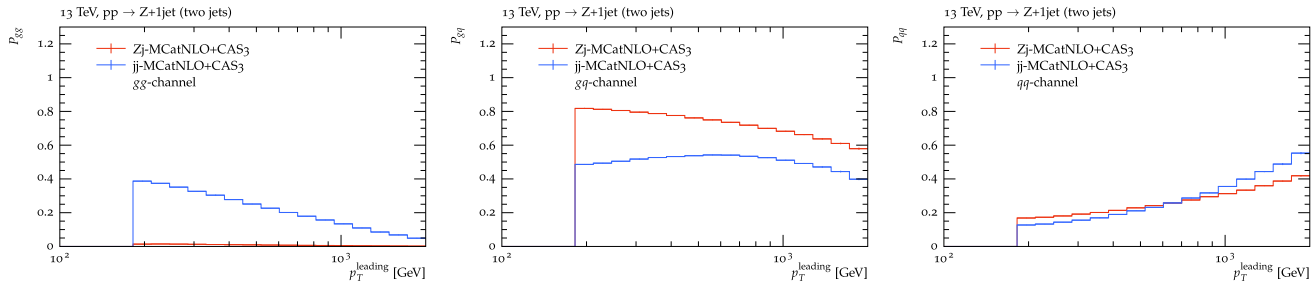

Fig. 4 The probability of gg, qg and qq initial states in Z+jet and multijet production (q stands for quark and antiquark) as a function of $p_{\mathrm{T}}^{\mathrm{leading}}$. The predictions are calculated with MCatNLO+CAS3

tion MCatNLO+Pythia8 we apply the Pythia8 subtraction terms in the MadGraph5_aMC@NLO calculation, use the NNPDF3.0 [82] parton density and tune CUETP8M1 [83].

As shown in Fig. 5, the distributions are different because of the different parton shower in Cascade3 and Pythia8, but the ratio of the distributions for Z+jet and multijet production are similar: Z+jet-production gives a steeper (more strongly correlated) distribution at low $p_{\mathrm{T}}^{\mathrm{leading}}$, while at high $p_{\mathrm{T}}^{\mathrm{leading}}$ the distributions become similar in shape. We conclude, that the main effect of the $\Delta\phi$ decorrelation comes from initial state radiation, and the shape of the $\Delta\phi$ decorrelation in the back-to-back region becomes similar between Z+jet and dijet processes at high $p_{\mathrm{T}}^{\mathrm{leading}}$ where similar initial partonic states are important.

The matching scale μ_m limits the hardness of parton-shower emissions, and is thus typically a non-negligible source of variation in matched calculations (see e.g. [84] for a detailed discussion). It is thus interesting to assess the robustness of the previous findings under variations of the matching scale. Assessing matching scale variations in both an angular-ordered shower – such as Cascade3 – and a transverse-momentum-ordered shower – such as Pythia8 – additionally tests the *interpretation (role)* of the matching scale. In transverse-momentum ordered showers, the matching scale sets the maximal transverse momentum of the first shower branchings, while branchings beyond the first emission are not explicitly affected by the matching scale. In an angular-ordered shower, however, the matching scale is applied as "veto scale" to avoid larger transverse momenta for any branching, i.e. the matching scale directly affects all branchings. The result of changing the matching scale to half or twice the central value is shown in Fig. 6. As expected, the value of the matching scale has an impact on the prediction ($\sim 5\%$). This is particularly apparent when μ_m is used to set the maximal transverse momentum of the first emission in Pythia8. Overall, we find that interpreting the matching scale as veto scale in Cascade3 leads to apparently more robust predictions. Interestingly, the matching scale uncertainty becomes smaller for higher-$p_{\mathrm{T}}^{\mathrm{leading}}$ jet configurations in Cascade3. The size of the matching scale variation is comparable to scale variations, and should thus be carefully studied when designing uncertainty estimates.

In dijet production the measurements are rather well described with predictions obtained with MCatNLO+CAS3, as shown in Fig. 3 and discussed in detail in Ref. [23]. Only in the very high $p_{\mathrm{T}}^{\mathrm{leading}}$ region, a deviation from the mea-

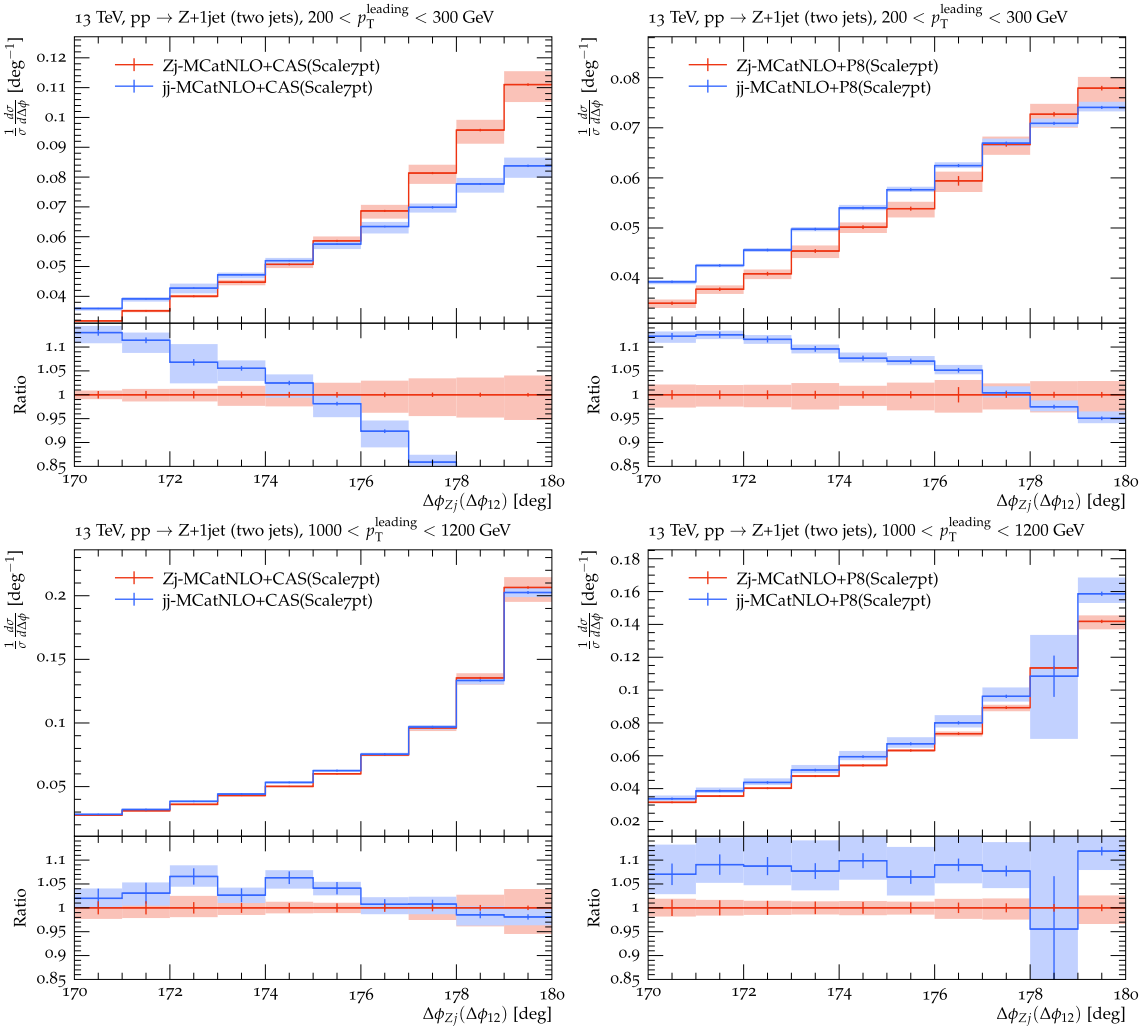

Fig. 5 Predictions for the azimuthal correlation $\Delta\phi_{\mathrm{Zj}}(\Delta\phi_{12})$ in the back-to-back region for Z+jet and multijet production obtained with MCatNLO+CAS3 (left column) and MCatNLO+PYTHIA8 (right column). Shown are different regions in $p_{\mathrm{T}}^{\mathrm{leading}} > 200$ GeV (upper row) and $p_{\mathrm{T}}^{\mathrm{leading}} > 1000$ GeV (lower row). The bands show the uncertainties obtained from scale variation (as described in the text)

surement is observed, which could be perhaps interpreted as coming from a violation of factorization. It is therefore very important to measure $\Delta\phi$ distributions in other processes, where factorization is expected to hold.

In order to experimentally probe effects which could originate from factorization-breaking in the back-to-back region we propose to measure the ratio of distributions in $\Delta\phi_{\mathrm{Zj}}$ for Z+jet and $\Delta\phi_{12}$ for multijet production at low and very high $p_{\mathrm{T}}^{\mathrm{leading}}$, and compare the measurement with predictions assuming that factorization holds. The number of colored partons involved in Z+jet and multijet events is different, and deviations from factorization will depend on the structure of the colored initial and final state. In order to minimize the effect of different initial state configurations, a measurement at high $p_{\mathrm{T}}^{\mathrm{leading}}$, hint more clearly at possible factorization-breaking effects.

In Ref. [11] a detailed study on Z+jet azimuthal correlations is reported, applying TMD-factorization and the "winner-takes-all" jet recombination scheme, with the aim to reduce potential factorization breaking contributions. We have checked that our main results remain largely unchanged when the "winner-takes-all" jet recombination scheme [85, 86] is applied and only in the last bin of the $\Delta\phi_{\mathrm{Zj}}$ distributions the cross section is reduced. We find that multijet events are more affected by the "winner-takes-all" jet recombination scheme in the back-to-back region at high p_{T} than Z+jet events.

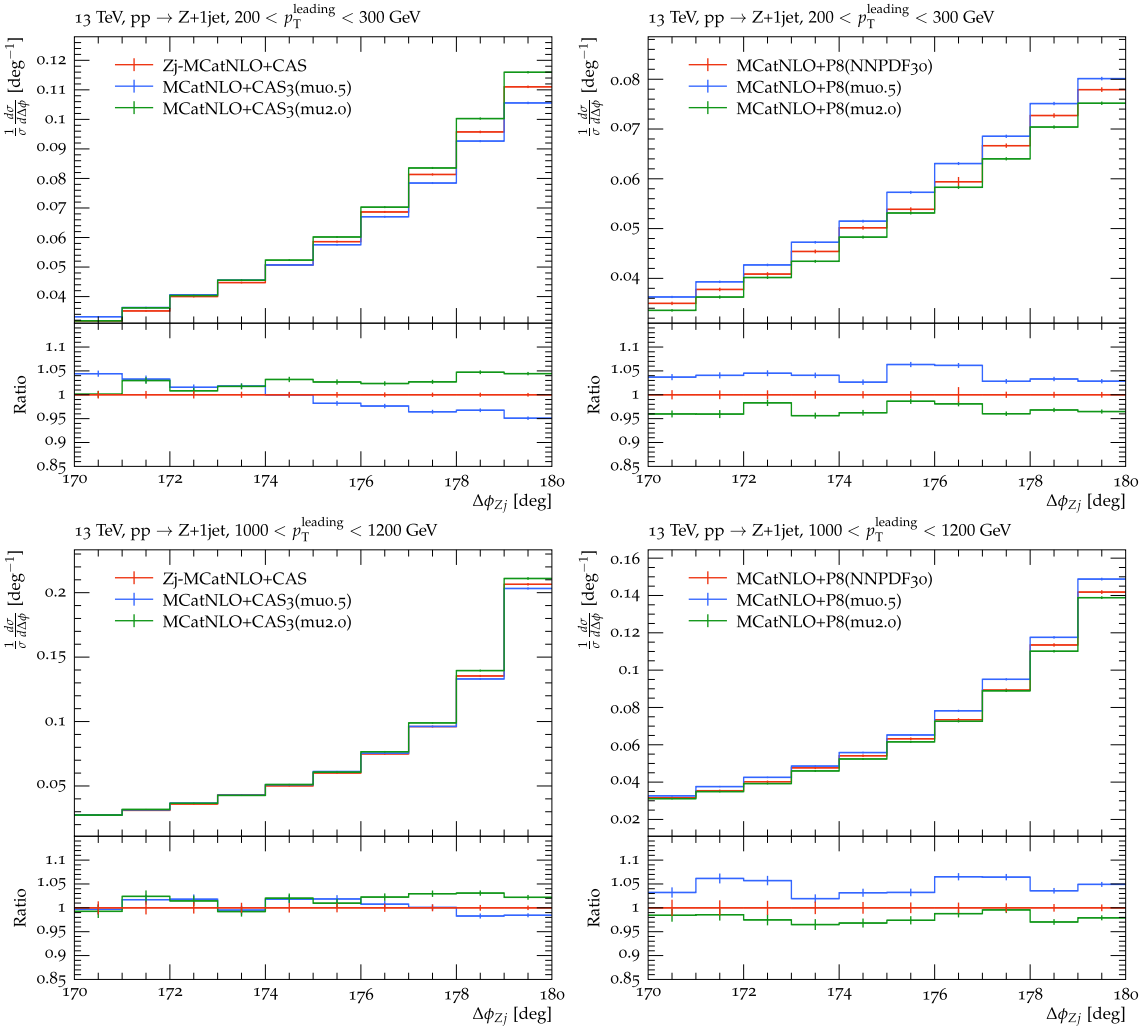

Fig. 6 The dependence on the variation of the matching scale μ_m in predictions for the azimuthal correlation $\Delta\phi_{\mathrm{Zj}}(\Delta\phi_{12})$ in the back-to-back region. Shown are predictions obtained with MCatNLO+CAS3 (left column) and MCatNLO+PYTHIA8 (right column) for $p_{\mathrm{T}}^{\mathrm{leading}} >$ 200 GeV (upper row) and $p_{\mathrm{T}}^{\mathrm{leading}} > 1000$ GeV (lower row). The predictions with different matching scales μ_m varied by a factor of two up and down are shown

4 Summary and conclusions

We have investigated azimuthal correlations in Z+jet production and compared predictions with those for multijet production in the same kinematic range. The predictions are based on PB-TMD distributions with NLO calculations via MCatNLO supplemented by PB-TMD parton showers via CASCADE3. The azimuthal correlations $\Delta\phi_{\mathrm{Zj}}$, obtained in Z+jet production are steeper compared to those in multijet production ($\Delta\phi_{12}$) at transverse momenta $\mathcal{O}(100)$ GeV, while they become similar for very high transverse momenta, $\mathcal{O}(1000)$ GeV, which is a result of similar initial parton configuration of both processes.

In Z+jet production the color and spin structure of the partonic final state is different compared to the one in multijet production, and differences in the azimuthal correlation patterns can be used to search for potential factorization - breaking effects, involving initial and final state interferences. In order to experimentally investigate those effects, we propose to measure the ratio of the distributions in $\Delta\phi_{\mathrm{Zj}}$ for Z+jet- and $\Delta\phi_{12}$ for multijet production at low and at very high $p_{\mathrm{T}}^{\mathrm{leading}}$, and compare the measurements to predictions obtained assuming that factorization holds.

We have studied the matching scale dependence in the PB-TMD predictions and compared it with the case of NLO-matched calculations based on the PYTHIA8 collinear shower. We find that variations of the matching scale lead to more stable predictions in the PB-TMD case, with the relative reduction of the matching scale theoretical uncertainty becoming more pronounced for increasing $p_{\mathrm{T}}^{\mathrm{leading}}$ transverse momenta.

Acknowledgements We are grateful to Olivier Mattelaer from the MADGRAPH5_AMC@NLO team for discussions, help and support with the LHE option for fixed NLO calculations in MCatNLO.

Data Availability Statement This manuscript has no associated data or the data will not be deposited. [Authors' comment: This is a phenomenological study without producing experimental data. The results of the Monte Carlo simulations are presented in the figures.]

Funded by SCOAP^3. SCOAP^3 supports the goals of the International Year of Basic Sciences for Sustainable Development.

Appendix: Comparison of CASCADE3 and HERWIG6

The calculations presented here apply the MCatNLO method using HERWIG6 (H6) subtraction terms, as implemented in MADGRAPH5_AMC@NLO. The NLO accuracy of the calculations is preserved by construction, since the use of PB-TMD distributions and TMD shower, as well as the ordinary parton shower, does not change the inclusive cross section.

Since HERWIG6 (H6) subtraction terms are used in the MCatNLO+CAS3 calculations, we investigate here in detail the contribution of the parton shower used in CASCADE3. We compare predictions obtained with MCatNLO+CAS3 with the corresponding ones obtained with MCatNLO+H6, using LHE files produced with MADGRAPH5_AMC@NLO for Z production. The Z boson is reconstructed from two oppositely charged leptons with $p_T > 20$ GeV in $|\eta| < 2.4$. We also study jet distributions obtained with the anti-k_T algorithm with distance parameter 0.4 with $p_T > 30$ GeV and $|\eta| < 5$.

In H6 the allowed region of z for a branching $q \to qg$ in the final state shower is $Q_q/Q < z < 1 - Q_g/Q$ (e.g. A.2.2 in Ref. [87]), with $Q_q = m_q + \texttt{VQCUT}$ and $Q_g = m_g + \texttt{VGCUT}$, and m_q, m_g being the quark and gluon effective masses, and `VQCUT`, `VGCUT` the minimum virtuality parameters. Similar cuts are applied for initial state shower.

First we investigate final state parton showers. We compare distributions of the first and second jet in Z+jet events: the first (highest p_T) jet is part of the lowest order process, while the second (highest p_T) jet is the real correction and therefore subject to subtraction terms (keeping in mind that the highest p_T jet in the NLO calculation can also come from the α_s^2 real emission diagram). In CASCADE3, the PYTHIA6 final state shower is used (since the PB-method has not yet been applied for final state radiation), with the angular ordering veto condition. Since final state radiation is independent of parton densities, a direct comparison of MCatNLO+CAS3 and MCatNLO+H6, using the same LHE files, while only simulating final state radiation, is possible. In Fig. 7 we show a comparison of predictions for the transverse momentum of the first two highest p_T jets in Z+jet events (using identical LHE files).

The uncertainty coming from different parameter settings in the H6 final state parton shower is estimated by changing the light quark masses from the default to 0.32 GeV (`Rmas =`

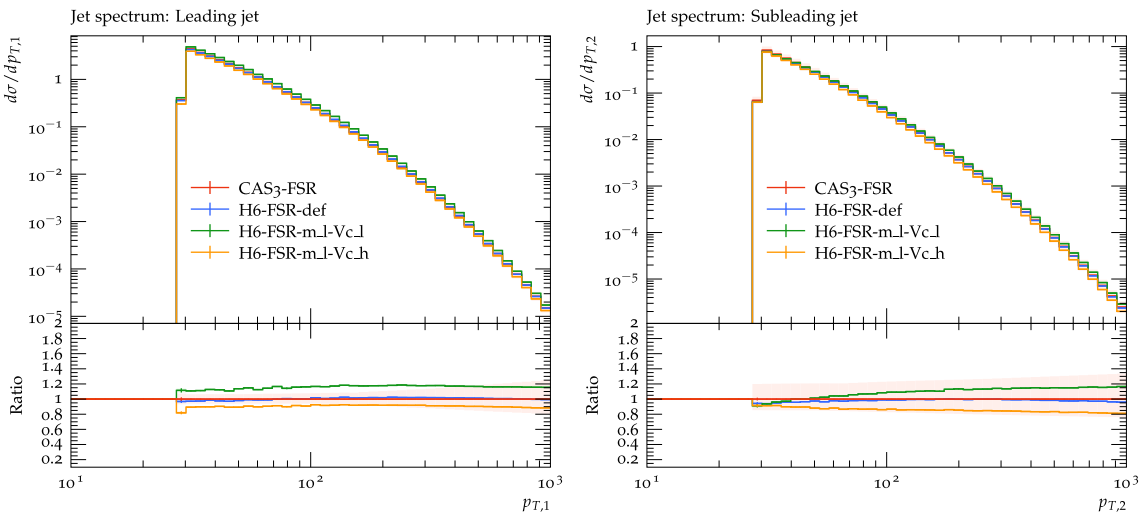

Fig. 7 Comparison of predictions obtained with MCatNLO+CAS3 and MCatNLO+H6 for Z+jet obtained with MCatNLO. Shown are predictions using only final state parton shower. The band of MCatNLO+CAS3 shows the uncertainties obtained from scale variation (as described in the text)

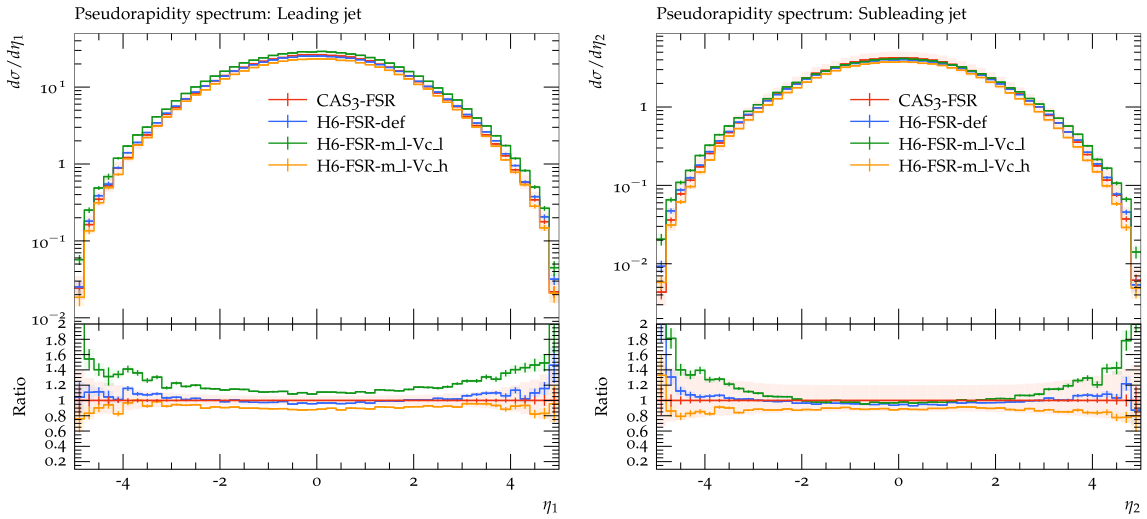

Fig. 8 Comparison of predictions obtained with MCatNLO+CAS3 and MCatNLO+H6 for Z+jet obtained with MCatNLO. Shown are predictions using only final state parton shower. The band of MCatNLO+CAS3 shows the uncertainties obtained from scale variation (as described in the text)

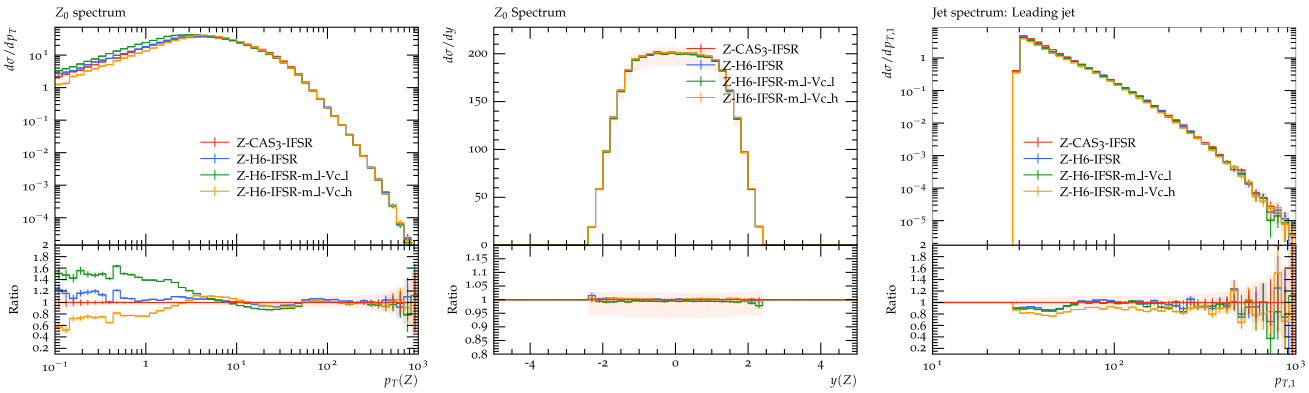

Fig. 9 Comparison of predictions obtained with MCatNLO+CAS3 and MCatNLO+H6 for Z production obtained with MCatNLO. Shown are predictions using initial state parton shower. The band of MCatNLO+CAS3 shows the uncertainties obtained from scale variation (as described in the text)

`0.32`, labelled as m_l) and `VQCUT`, `VGCUT` from the default to `0.1(1.5)`, labelled as $Vc_l(Vc_h)$, respectively (the lowest values chosen are those for which H6 is still working).

In Fig. 8 a comparison is shown for the pseudorapidity η of the first two highest p_T jets. Within the variation of the parameters, the prediction of MCatNLO+CAS3 agrees well with the one of MCatNLO+H6, justifying the application of the PYTHIA6 final state parton shower algorithm.

Next we investigate the contribution of PB-TMD PDFs and the PB-TMD parton shower in the initial state and compare the predictions with the ones from H6. We study Z production generated by MADGRAPH5_aMC@NLO which is essentially driven by initial state radiation. In Fig. 9 we show the transverse momentum of the Z boson, its rapidity distribution and the transverse momentum of the first reconstructed jet with $p_T > 30$ GeV and $|\eta| < 5$. Here the rapidity y of the Z boson is used, since it is related to the momentum fractions of the initial partons (instead of the pseudorapidity η which is used for jets as it is related to the scattering angle θ). We show a comparison of MCatNLO+CAS3 and MCatNLO+H6 predictions (including the same parameter variations for H6 as for the final state shower). In the region of low transverse momentum of the Z boson one can clearly see the sensitivity to the parameter choice in H6.

While at low p_T the parton shower matters, and the CAS3 prediction lies in between the ones from H6 with parameter variation, we observe good matching of the parton shower to the real emission at higher transverse momentum. The rapidity distribution obtained from CAS3 also lies within the one predicted by H6 with parameter variation. The p_T distribution of the first jet also agrees well within the band given by the uncertainties.

Finally we investigate Z+jet events, when both initial and final state radiation is important. In Fig. 10 we show a comparison of MCatNLO+CAS3 and MCatNLO+H6 predictions (including the same parameter variations for H6 as for the

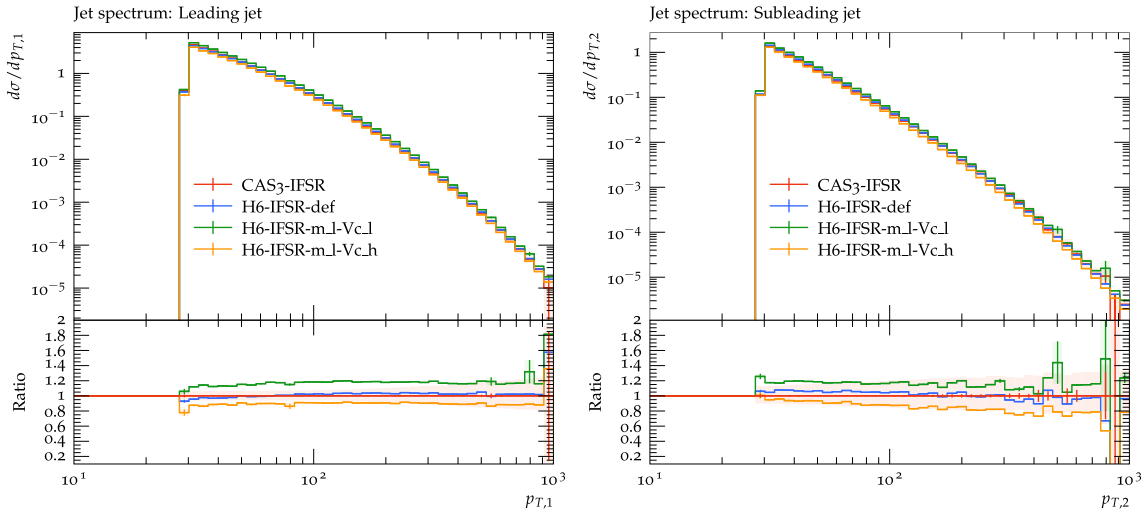

Fig. 10 Comparison of predictions obtained with MCatNLO+CAS3 and MCatNLO+H6 for Z+jet obtained with MCatNLO. Shown are predictions using initial and final state parton shower. The band of MCatNLO+CAS3 shows the uncertainties obtained from scale variation (as described in the text)

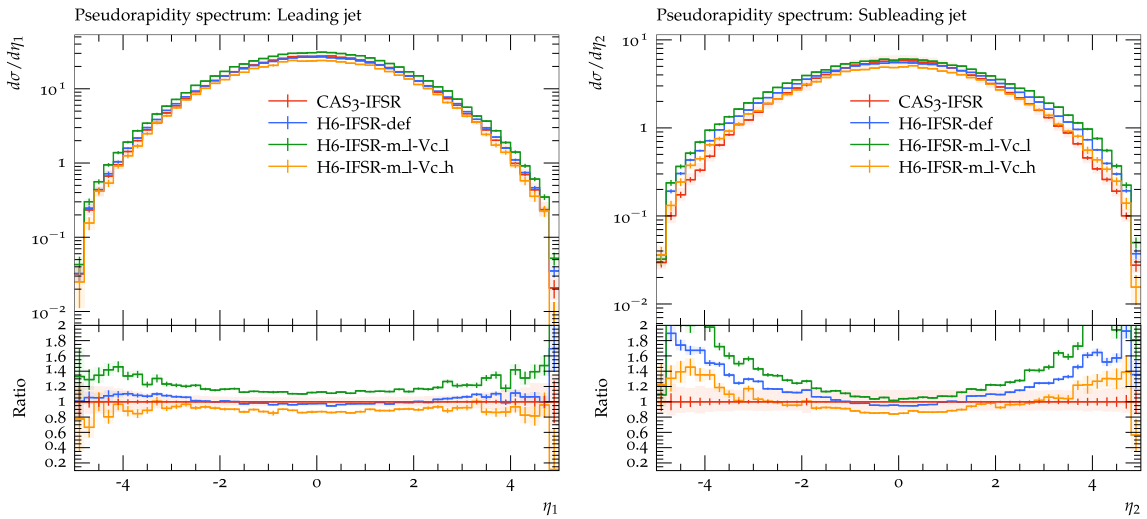

Fig. 11 Comparison of predictions obtained with MCatNLO+CAS3 and MCatNLO+H6 for Z+jet obtained with MCatNLO. Shown are predictions using initial and final state parton shower. The band of MCatNLO+CAS3 shows the uncertainties obtained from scale variation (as described in the text)

final state shower) for the transverse momentum of the first two highest p_T jets. In Fig. 11 the corresponding comparison is shown for the pseudorapidity distributions. The transverse momentum distributions agree well within the uncertainties coming from parameter variations, while for the η-distributions some differences in the very forward/backward regions are seen. However, one can see, that a variation of `VQCUT`, `VGCUT` has a significant effect especially in the forward/backward region.

In conclusion, we observe agreement between predictions obtained by MCatNLO+CAS3 and MCatNLO+H6 within the band of parton shower parameter variation in H6, confirming the use of H6 subtraction terms in MCatNLO together with PB - TMD PDFs, and PB - TMD initial state parton shower, as applied in MCatNLO+CAS3.

References

1. CDF Collaboration, Measurement of inclusive jet cross-sections in $Z/\gamma^* \to e^+e^-$ + jets production in $p\bar{p}$ collisions at $\sqrt{s}$ = 1.96-TeV. Phys. Rev. Lett. **100**, 102001 (2008). arXiv:0711.3717
2. D0 Collaboration, Measurement of differential Z/γ^* + jet + X cross sections in $p\bar{p}$ collisions at $\sqrt{s}$ = 1.96-TeV. Phys. Lett. B **669**, 278–286 (2008). arXiv:0808.1296
3. ATLAS Collaboration, Measurement of the production cross section of jets in association with a Z boson in pp collisions at

$\sqrt{s}$ = 7 TeV with the ATLAS detector. JHEP **07**, 032 (2013). arXiv:1304.7098
4. ATLAS Collaboration, Measurement of the production cross section for Z/γ^* in association with jets in pp collisions at $\sqrt{s}$ = 7 TeV with the ATLAS detector. Phys. Rev. D **85**, 032009 (2012). arXiv:1111.2690
5. CMS Collaboration, Measurements of jet multiplicity and differential production cross sections of $Z+$ jets events in proton–proton collisions at $\sqrt{s} = 7$ TeV. Phys. Rev. D **91**, 052008 (2015). arXiv:1408.3104
6. CMS Collaboration, Measurements of differential production cross sections for a Z boson in association with jets in pp collisions at $\sqrt{s} = 8$ TeV. JHEP **04**, 022 (2017). arXiv:1611.03844
7. ATLAS Collaboration, Measurements of the production cross section of a Z boson in association with jets in pp collisions at $\sqrt{s} = 13$ TeV with the ATLAS detector. Eur. Phys. J. C **77**, 361 (2017). arXiv:1702.05725
8. CMS Collaboration, Measurement of differential cross sections for Z boson production in association with jets in proton–proton collisions at $\sqrt{s}$ = 13 TeV. Eur. Phys. J. C **78**, 965 (2018). arXiv:1804.05252
9. R. Angeles-Martinez et al., Transverse Momentum Dependent (TMD) parton distribution functions: status and prospects. Acta Phys. Pol. B **46**(12), 2501 (2015). arXiv:1507.05267
10. H. Bouaziz, Y. Delenda, K. Khelifa-Kerfa, Azimuthal decorrelation between a jet and a Z boson at hadron colliders. arXiv:2207.10147
11. Y.-T. Chien et al., Precision boson-jet azimuthal decorrelation at hadron colliders. arXiv:2205.05104
12. L. Buonocore, M. Grazzini, J. Haag, L. Rottoli, Transverse-momentum resummation for boson plus jet production at hadron colliders. Eur. Phys. J. C **82**, 27 (2022). arXiv:2110.06913
13. Y.-T. Chien et al., Recoil-free azimuthal angle for precision boson-jet correlation. Phys. Lett. B **815**, 136124 (2021). arXiv:2005.12279
14. Y.-T. Chien, D.Y. Shao, B. Wu, Resummation of boson-jet correlation at hadron colliders. JHEP **11**, 025 (2019). arXiv:1905.01335
15. M.G.A. Buffing, Z.-B. Kang, K. Lee, X. Liu, A transverse momentum dependent framework for back-to-back photon+jet production. arXiv:1812.07549
16. P. Sun, B. Yan, C.P. Yuan, F. Yuan, Resummation of high order corrections in Z boson plus jet production at the LHC. Phys. Rev. D **100**, 054032 (2019). arXiv:1810.03804
17. F. Hautmann et al., Soft-gluon resolution scale in QCD evolution equations. Phys. Lett. B **772**, 446 (2017). arXiv:1704.01757
18. F. Hautmann et al., Collinear and TMD quark and gluon densities from Parton Branching solution of QCD evolution equations. JHEP **01**, 070 (2018). arXiv:1708.03279
19. J. Alwall et al., The automated computation of tree-level and next-to-leading order differential cross sections, and their matching to parton shower simulations. JHEP **1407**, 079 (2014). arXiv:1405.0301
20. A. Bermudez Martinez et al., Production of Z-bosons in the parton branching method. Phys. Rev. D **100**, 074027 (2019). arXiv:1906.00919
21. A. Bermudez Martinez et al., The transverse momentum spectrum of low mass Drell–Yan production at next-to-leading order in the parton branching method. Eur. Phys. J. C **80**, 598 (2020). arXiv:2001.06488
22. F. Hautmann, I. Scimemi, A. Vladimirov, Non-perturbative contributions to vector-boson transverse momentum spectra in hadronic collisions. Phys. Lett. B **806** 135478 (2020)
23. M.I. Abdulhamid et al., Azimuthal correlations of high transverse momentum jets at next-to-leading order in the parton branching method. Eur. Phys. J. C **82**, 36 (2022). arXiv:2112.10465
24. ATLAS Collaboration, Measurement of dijet azimuthal decorrelations in pp collisions at sqrt(s) = 7 TeV. Phys. Rev. Lett. **106**, 172002 (2011). arXiv:1102.2696
25. CMS Collaboration, Dijet azimuthal decorrelations in pp collisions at sqrt(s) = 7 TeV. Phys. Rev. Lett. **106**, 122003 (2011). arXiv:1101.5029
26. CMS Collaboration, Measurement of dijet azimuthal decorrelation in pp collisions at $\sqrt{s} = 8$ TeV. Eur. Phys. J. C **76**, 536 (2016). arXiv:1602.04384
27. CMS Collaboration, Azimuthal correlations for inclusive 2-jet, 3-jet, and 4-jet events in pp collisions at $\sqrt{s} = 13$ TeV. Eur. Phys. J. C **78**, 566 (2018). arXiv:1712.05471
28. CMS Collaboration, Azimuthal separation in nearly back-to-back jet topologies in inclusive 2- and 3-jet events in pp collisions at $\sqrt{s} = 13$ TeV. Eur. Phys. J. C **79**, 773 (2019). arXiv:1902.04374
29. J. Collins, J.-W. Qiu, k_T factorization is violated in production of high-transverse-momentum particles in hadron–hadron collisions. Phys. Rev. D **75**, 114014 (2007). arXiv:0705.2141
30. W. Vogelsang, F. Yuan, Hadronic dijet imbalance and transverse-momentum dependent parton distributions. Phys. Rev. D **76**, 094013 (2007). arXiv:0708.4398
31. T.C. Rogers, P.J. Mulders, No generalized TMD-factorization in hadro-production of high transverse momentum hadrons. Phys. Rev. D **81**, 094006 (2010). arXiv:1001.2977
32. T.C. Rogers, Extra spin asymmetries from the breakdown of transverse-momentum-dependent factorization in hadron–hadron collisions. Phys. Rev. D **88**, 014002 (2013). arXiv:1304.4251
33. V.N. Gribov, L.N. Lipatov, Deep inelastic ep scattering in perturbation theory. Sov. J. Nucl. Phys. **15**, 438 (1972) [Yad. Fiz. **15**, 781 (1972)]
34. L.N. Lipatov, The parton model and perturbation theory. Sov. J. Nucl. Phys. **20**, 94 (1975) [Yad. Fiz. **20**, 181 (1974)]
35. G. Altarelli, G. Parisi, Asymptotic freedom in parton language. Nucl. Phys. B **126**, 298 (1977)
36. Y.L. Dokshitzer, Calculation of the structure functions for Deep Inelastic Scattering and e^+e^- annihilation by perturbation theory in Quantum Chromodynamics. Sov. Phys. JETP **46**, 641 (1977) [Zh. Eksp. Teor. Fiz. **73**, 1216 (1977)]
37. G. Marchesini, B.R. Webber, Monte Carlo simulation of general hard processes with coherent QCD radiation. Nucl. Phys. B **310**, 461 (1988)
38. S. Catani, B.R. Webber, G. Marchesini, QCD coherent branching and semiinclusive processes at large x. Nucl. Phys. B **349**, 635 (1991)
39. F. Hautmann, L. Keersmaekers, A. Lelek, A.M. Van Kampen, Dynamical resolution scale in transverse momentum distributions at the LHC. Nucl. Phys. B **949**, 114795 (2019). arXiv:1908.08524
40. B.R. Webber, Monte Carlo simulation of hard hadronic processes. Ann. Rev. Nucl. Part. Sci. **36**, 253–286 (1986)
41. J. Bellm et al., Herwig 7.0/Herwig++ 3.0 release note. Eur. Phys. J. C **76**, 196 (2016). arXiv:1512.01178
42. T. Sjöstrand et al., An introduction to PYTHIA 8.2. Comput. Phys. Commun. **191**, 159 (2015). arXiv:1410.3012
43. S. Baranov et al., CASCADE3 a Monte Carlo event generator based on TMDs. Eur. Phys. J. C **81**, 425 (2021). arXiv:2101.10221
44. A. Bermudez Martinez et al., Collinear and TMD parton densities from fits to precision DIS measurements in the parton branching method. Phys. Rev. D **99**, 074008 (2019). arXiv:1804.11152
45. ZEUS, H1 Collaboration, Combination of measurements of inclusive deep inelastic $e^{\pm}p$ scattering cross sections and QCD analysis of HERA data. Eur. Phys. J. C **75**, 580 (2015). arXiv:1506.06042
46. xFitter Developers' Team Collaboration, H. Abdolmaleki et al., xFitter: an open source QCD analysis framework. A resource and reference document for the Snowmass study (2022). arXiv:2206.12465

47. S. Alekhin et al., HERAFitter. Eur. Phys. J. C **75**, 304 (2015). arXiv:1410.4412
48. A. Bassetto, M. Ciafaloni, G. Marchesini, Jet structure and infrared sensitive quantities in perturbative QCD. Phys. Rep. **100**, 201–272 (1983)
49. Y.L. Dokshitzer, V.A. Khoze, S.I. Troian, A.H. Mueller, QCD coherence in high-energy reactions. Rev. Mod. Phys. **60**, 373 (1988)
50. A.M. van Kampen, Drell-Yan transverse spectra at the LHC: a comparison of parton branching and analytical resummation approaches SciPost Phys. Proc. **8**, 151 (2022)
51. J.C. Collins, D.E. Soper, G.F. Sterman, Transverse momentum distribution in Drell–Yan pair and W and Z boson production. Nucl. Phys. B **250**, 199 (1985)
52. J. Collins, *Foundations of Perturbative QCD. Cambridge Monographs on Particle Physics, Nuclear Physics and Cosmology*, vol. 32 (2011)
53. A. Bacchetta et al., Unpolarized transverse momentum distributions from a global fit of Drell–Yan and semi-inclusive deep-inelastic scattering data. arXiv:2206.07598
54. M. Bury et al., PDF bias and flavor dependence in TMD distributions. arXiv:2201.07114
55. N.A. Abdulov et al., TMDlib2 and TMDplotter: a platform for 3D hadron structure studies. Eur. Phys. J. C **81**, 752 (2021). arXiv:2103.09741
56. F. Hautmann et al., TMDlib and TMDplotter: library and plotting tools for transverse-momentum-dependent parton distributions. Eur. Phys. J. C **74**(12), 3220 (2014). arXiv:1408.3015
57. ATLAS Collaboration, Measurement of the transverse momentum and ϕ_η^* distributions of Drell–Yan lepton pairs in proton–proton collisions at $\sqrt{s} = 8$ TeV with the ATLAS detector. Eur. Phys. J. C **76**, 291 (2016). arXiv:1512.02192
58. CMS Collaboration, Measurements of differential Z boson production cross sections in proton–proton collisions at $\sqrt{s} = 13$ TeV. JHEP **12**, 061 (2019). arXiv:1909.04133
59. CMS Collaboration, Measurement of the mass dependence of the transverse momentum of lepton pairs in Drell–Yan production in proton–proton collisions at $\sqrt{s} = 13$ TeV. arXiv:2205.04897
60. PHENIX Collaboration, Measurements of $\mu\mu$ pairs from open heavy flavor and Drell–Yan in $p + p$ collisions at $\sqrt{s} = 200$ GeV. Phys. Rev. D **99**, 072003 (2019). arXiv:1805.02448
61. D. Antreasyan et al., Dimuon scaling comparison at 44-GeV and 62-GeV. Phys. Rev. Lett. **48**, 302 (1982)
62. NuSea Collaboration, Absolute Drell–Yan dimuon cross sections in 800-GeV/c pp and pd collisions. arXiv:hep-ex/0302019
63. J.C. Webb, Measurement of continuum dimuon production in 800-GeV/c proton nucleon collisions. arXiv:hep-ex/0301031
64. R. Gauld et al., Transverse momentum distributions in low-mass Drell–Yan lepton pair production at NNLO QCD. Phys. Lett. B **829**, 137111 (2022). arXiv:2110.15839
65. A. Bermudez Martinez, F. Hautmann, M.L. Mangano, TMD evolution and multi-jet merging. Phys. Lett. B **822**, 136700 (2021). arXiv:2107.01224
66. A. Bermudez Martinez, F. Hautmann, M.L. Mangano, Multi-jet merging with TMD parton branching. arXiv:2208.02276
67. A. Bermudez Martinez, F. Hautmann, M.L. Mangano, Multi-jet physics at high-energy colliders and TMD parton evolution (2021). arXiv:2109.08173
68. F. Hautmann, QCD and jets. Acta Phys. Pol. B **44**, 761–778 (2013)
69. S. Dooling, P. Gunnellini, F. Hautmann, H. Jung, Longitudinal momentum shifts, showering and nonperturbative corrections in matched NLO-shower event generators. Phys. Rev. D **87**, 094009 (2013). arXiv:1212.6164
70. F. Hautmann, H. Jung, Collinearity approximations and kinematic shifts in partonic shower algorithms. Eur. Phys. J. C **72**, 2254 (2012). arXiv:1209.6549
71. F. Hautmann et al., A parton branching with transverse momentum dependent splitting functions. arXiv:2205.15873
72. L. Keersmaekers, Implementing transverse momentum dependent splitting functions in parton branching evolution equations. SciPost Phys. Proc. **8**, 127 (2022). arXiv:2109.07326
73. S. Catani, F. Hautmann, High-energy factorization and small x deep inelastic scattering beyond leading order. Nucl. Phys. B **427**, 475 (1994). arXiv:hep-ph/9405388
74. J. Alwall et al., A standard format for Les Houches event files. Comput. Phys. Commun. **176**, 300 (2007). arXiv:hep-ph/0609017
75. G. Corcella et al., HERWIG 6.5 release note. arXiv:hep-ph/0210213
76. G. Marchesini et al., HERWIG: a Monte Carlo event generator for simulating hadron emission reactions with interfering gluons. Version 5.1-April 1991. Comput. Phys. Commun. **67**, 465 (1992)
77. M. Cacciari, G.P. Salam, G. Soyez, The anti-k_t jet clustering algorithm. JHEP **04**, 063 (2008). arXiv:0802.1189
78. M. Cacciari, G.P. Salam, G. Soyez, FastJet user manual. Eur. Phys. J. C **72**, 1896 (2012). arXiv:1111.6097
79. H. Jung et al., The CCFM Monte Carlo generator CASCADE version 2.2.03. Eur. Phys. J. C **70**, 1237 (2010). arXiv:1008.0152
80. S. Dooling, F. Hautmann, H. Jung, Hadroproduction of electroweak gauge boson plus jets and TMD parton density functions. Phys. Lett. B **736**, 293 (2014). arXiv:1406.2994
81. F. Hautmann, H. Jung, Angular correlations in multi-jet final states from kt-dependent parton showers. JHEP **10**, 113 (2008). arXiv:0805.1049
82. NNPDF Collaboration, Parton distributions for the LHC Run II. JHEP **04**, 040 (2015). arXiv:1410.8849
83. CMS Collaboration, Event generator tunes obtained from underlying event and multiparton scattering measurements. Eur. Phys. J. C **76**, 155 (2016). arXiv:1512.00815
84. J. Bellm et al., Parton shower uncertainties with Herwig 7: benchmarks at leading order. Eur. Phys. J. C **76**, 665 (2016). arXiv:1605.01338
85. G. Salam, E_t^∞ scheme. Unpublished
86. D. Bertolini, T. Chan, J. Thaler, Jet observables without jet algorithms. JHEP **04**, 013 (2014). arXiv:1310.7584
87. S. Frixione, P. Nason, B.R. Webber, Matching NLO QCD and parton showers in heavy flavour production. JHEP **08**, 007 (2003). arXiv:hep-ph/0305252